IET Microwaves, Antennas & Propagation

Research Article

IET Journals
The Institution of Engineering and Technology

Transverse slot with control of amplitude and phase for travelling-wave SIW antenna arrays

ISSN 1751-8725
Received on 23rd January 2020
Revised 11th July 2020
Accepted on 21st August 2020
E-First on 22nd October 2020
doi: 10.1049/iet-map.2020.0069
www.ietdl.org

Tomas Mikulasek[1] ✉, Jan Puskely[2], Alexander G. Yarovoy[2], Jaroslav Lacik[1], Holger Arthaber[3]

[1]*Department of Radio Electronics, Brno University of Technology, Technicka 12, 616 00 Brno, Czech Republic*
[2]*Delft University of Technology, Delft 2628, Netherlands*
[3]*Institute of Electrodynamics, Microwave and Circuit Engineering, Technische Universität Wien, 1040 Vienna, Austria*
✉ *E-mail: mikulasekt@feec.vutbr.cz*

Abstract: A novel basic antenna element for travelling-wave substrate integrated waveguide (SIW) arrays is proposed in this study. The antenna element is based on a transverse slot and newly complemented by a pair of vias used for matching and a phase shifter. By changing the geometries of the slot and the phase shifter, the amplitude and phase of a radiated wave can be controlled. The proposed approach extends the potential of transverse slots in SIW-based travelling-wave antenna arrays. To verify the capabilities of the antenna element, the authors demonstrate a six-element array with −30 dB side-lobe suppression, intended for a 24 GHz radar system. The measured results show good agreement with simulations.

1 Introduction

Substrate integrated waveguide (SIW) slot antenna arrays allow a large variety of slot configurations and feeding techniques and have been extensively studied in recent years [1–8]. Arrays are classified into two different types: standing-wave and travelling-wave arrays. In standing wave arrays, slots are spaced by half a wavelength and the waveguide is shorted after the last slot. In this configuration, the radiation pattern is strictly broadside and symmetric but it does not allow to control the phase distribution. On the other hand, travelling-wave arrays allow to achieve non-broadside and asymmetrical radiation patterns and a wider impedance bandwidth compared to the standing wave approach. The most common configuration for slot array antennas is the longitudinal placement of the slots in parallel to the SIW axis, based on Elliott's design procedure [9] in connection with full-wave analysis. So far, less attention has been paid to transverse slot arrays, due to their lower gain compared to longitudinal slot arrays of the same size.

Various antenna elements especially for longitudinal slot travelling-wave SIW arrays have been published. In [1], a travelling-wave array with non-uniformly spaced longitudinal slots was designed using Elliott's design formulas and optimisation algorithms. This ten-element antenna array achieved a 25° main beam inclination and a side lobe level (SLL) of −20 dB. Recently, two travelling-wave longitudinal slot arrays were proposed for a similar main beam inclination and a lower SLL in [2, 3]. An impedance bandwidth enhancement of the longitudinal slot travelling-wave SIW array was introduced using a double-layer cavity in [4]. The bandwidth was improved by a double-resonant feature of the cavity. In a series-fed travelling wave array, every antenna element radiates a part of the travelling wave going through the waveguide. Therefore, it is important to suppress reflected waves which would excite previous slots and thus decrease the entire array performance. Several methods for suppressing these reflections have been published. The most common technique uses an inductive post inserted into a waveguide near to a longitudinal slot antenna element [5], a transverse slot antenna element [6], or a 45° polarised slot antenna element [7]. In [6], one reflection-cancelling post is placed into a hollow waveguide near a transverse slot. The slot excites parasitic dipoles that are placed on a suspended dielectric layer. This structure can be only used for a uniform amplitude and phase distribution. In addition, the array is rather complicated for a circuit integration due to a metal waveguide. A different reflection-cancelling technique uses a pair of transverse slots. In [8], an unequally spaced 16-element array radiating a cosecant-shaped pattern was proposed. The two parallel slots control the radiated power and ensure a low-input reflection while the phase of the radiating wave is controlled by the spacing between the elements. It is obvious that the design of the antenna element can be rather complicated because the amplitude and phase of the radiated wave depend on all parameters of the pair of the slots. Further, the phase distribution has the limits and not every distribution can be realised.

To overcome the aforesaid problems, we propose a novel basic antenna element based on a transverse slot for a uniformlyspaced travelling-wave array. The transverse slot is complemented by a pair of reflection-cancelling vias and a phase shifter. The proposed element is simpler than comparable techniques as it allows controlling magnitude/phase by means of simple geometry changes while maintaining the element's overall length. In order to verify the capabilities of the proposed antenna element, a six-element antenna array with a −30 dB SLL is designed for a 24 GHz radar system.

2 Antenna element

This section describes the antenna element and its application to small uniformly spaced travelling-wave antenna arrays. The simulation results were achieved using the transient solver (finite integration technique) of CST Microwave Studio.

2.1 Element structure

The proposed antenna element is depicted in Fig. 1. It consists of a transverse slot complemented by a pair of metalised via holes representing a symmetrical iris, that compensates a capacitive reactance of the slot, and the phase shifter designed on a dielectric substrate Arlon 25N (ε_r = 3.37 and tan(δ) = 0.003 at 24 GHz) with a thickness t_{sub} of 0.76 mm. By numerical analysis of a single radiating element (Fig. 1*a*), the optimum geometry, the phase delay arg(S_{21}), and the coupling coefficient are derived and depicted in Fig. 2. The coupling coefficient C represents a ratio of the radiated power P_{rad} to the input power P_{in} and is expressed in terms of scattering parameters as

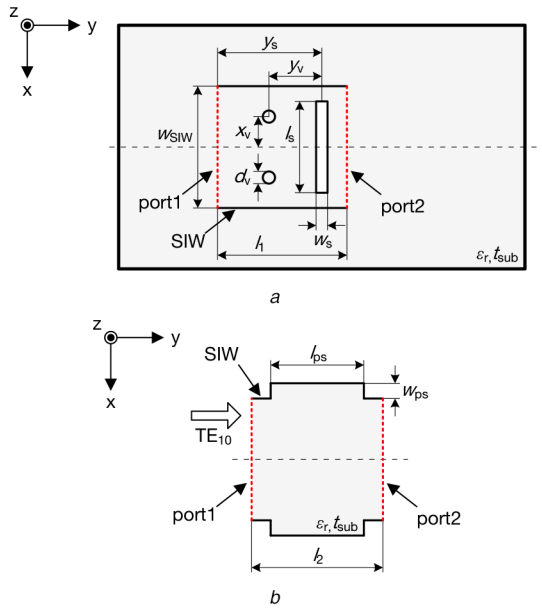

Fig. 1 *Configuration of proposed basic antenna element*
(a) Transverse slot with pair of metalised via holes, ***(b)*** Phase shifter

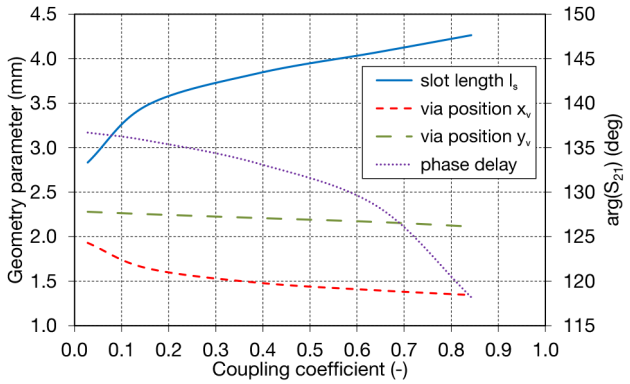

Fig. 2 *Geometry parameters and phase delay of transverse slot with pair of vias against coupling coefficient at 24.125 GHz*

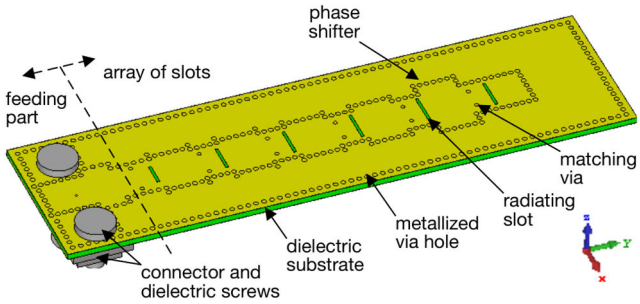

Fig. 3 *Structure of uniformly spaced slot antenna array*

$$C = \frac{P_{rad}}{P_{in}} = \frac{1 - |S_{11}|^2 - |S_{21}|^2}{1 - |S_{11}|^2}. \quad (1)$$

The coupling coefficient increases with the slot length l_s while the position x_v and y_v of the reflection-cancelling vias slightly changes. The phase delay decreases with growing coupling coefficient.

The phase of the travelling wave between adjacent antenna elements is controlled by the phase shifter (Fig. 1*b*) presented by the SIW discontinuity (l_{ps}, w_{ps}). The targeted total phase delay of 360° of the antenna element and phase shifter is achieved by changing the parameter w_{ps} of the phase shifter. The wider SIW leads to a smaller propagation constant and a higher phase shift. Hence, the transverse slot controls the amount of radiation power while the phase shifter controls the phase of the transmitted wave. The design curves are valid for the dielectric substrate Arlon 25N

Table 1 Coupling coefficients and geometry parameters of array elements, dimensions in millimetres

n	*C*	l_s	x_v	y_v	w_{ps}
1	0.03	2.83	1.93	2.28	0.35
2	0.16	3.48	1.64	2.25	0.36
3	0.39	3.84	1.48	2.21	0.46
4	0.64	4.07	1.40	2.17	0.72
5	0.84	4.26	1.34	2.11	1.58
6	1.00	3.97	1.31	2.34	

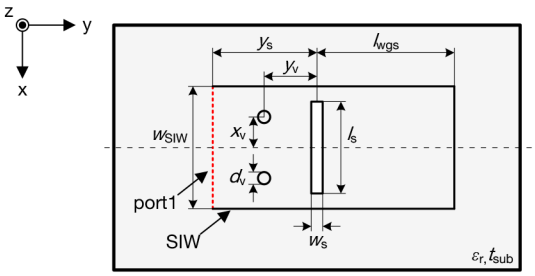

Fig. 4 *Configuration of radiating matched load*

and an SIW width $w_{SIW} = 5.10$ mm. The dielectric-filled SIW is assumed to have solid metal walls (instead of via rows) for reducing the computational costs of the simulation. It has an equivalent propagation constant and operates in the fundamental TE_{10} mode with the cutoff frequency of about 16 GHz as the via row-based SIW.

2.2 Array application

To validate the proposed antenna element operation, we design the uniformly spaced antenna array shown in Fig. 3 for a 24 GHz ISM band (250 MHz bandwidth at centre frequency of 24.125 GHz) and Dolph–Chebyshev amplitude distribution of 0.30–0.68–1.00–1.00–0.68–0.30 which corresponds to −30 dB SLL. The antenna array with such parameters is suitable for 24 GHz radar application. The distribution determines the coupling coefficients of the transverse slots listed in Table 1 using [8]

$$C(n) = \frac{|A(n)|^2}{\sum_{i=n}^{N} |A(i)|^2}, \quad (2)$$

where $A(n)$ is the excitation coefficient of nth element. The array consists of a five-element travelling-wave slot array (based on Fig. 1) and a standing-wave radiating slot (Fig. 4) functioning as a matched load with the coupling coefficient $C = 1$. The input reflection coefficients of the antenna elements are depicted in Fig. 5. The reflection coefficient bandwidth of antenna element depends on the quality factor of the interaction between the pair of vias and the slot, which is different for different elements of the array. A shorter slot takes less power of the exciting travelling wave. With a higher coupling coefficient, the interaction between the pair of vias and the slot grows and as a result the quality factor also increases. On the contrary, the bandwidth of the antenna elements decreases with the growing coupling coefficient. The separation of the slots is 8.70 mm that corresponds to $0.7\lambda_0$ at the centre frequency. The phase shifters placed in between the slots ensure in-phase feeding of the slots. Table 1 summarises the dimensions of the array elements. Other parameters of the antenna array are $l_{ps} = 4.80$ mm, $l_1 = 3.50$ mm, $l_2 = 5.20$ mm, $l_{wgs} = 4.52$ mm, $w_s = 0.35$ mm and $y_s = 3.00$ mm.

Fig. 6 shows simulated *S*-parameters of the five-element travelling-wave slot array terminated by a waveguide port and the radiating matched load. The entire residual power of the forward travelling wave, which corresponds to the parameter S_{21}, is radiated by the last element. Consequently, this leads to improving the efficiency of the array compared with an array terminated on a dissipative matched load [10]. The minimum of the reflection

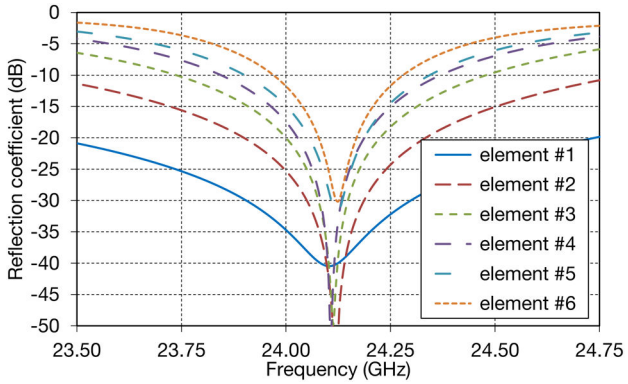

Fig. 5 *Reflection coefficients of antenna elements*

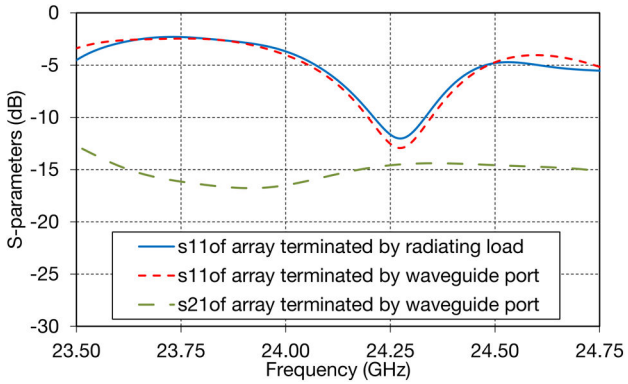

Fig. 6 *Simulated S-parameters of five-element travelling-wave slot array terminated by waveguide port and radiating matched load*

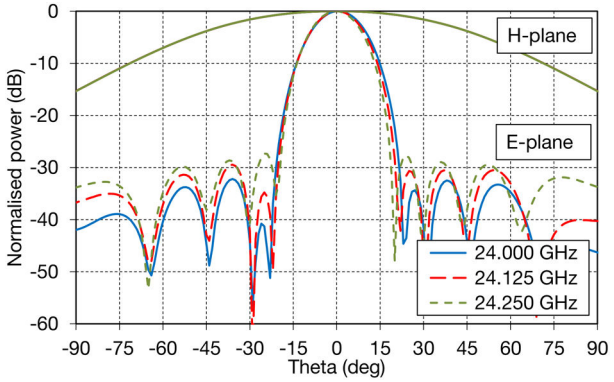

Fig. 7 *Normalised simulated radiation pattern of slot antenna array*

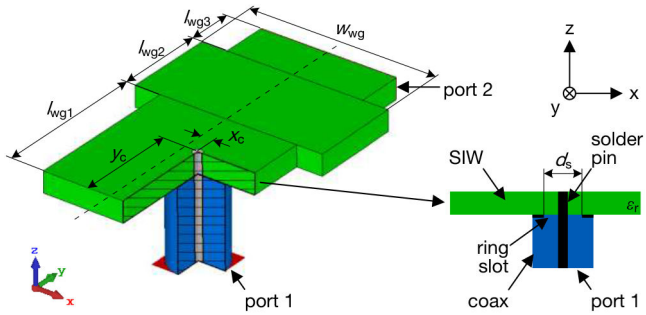

Fig. 8 *Configuration (left) and detail (right) of coax-to-SIW transition*

coefficient is slightly shifted as the design procedure is neglecting the mutual coupling between the elements. The bandwidth is rather narrow and results from the narrow-band feature of the antenna element (Fig. 5). The radiation pattern shown in Fig. 7 is stable over the 250 MHz bandwidth. Due to the narrow bandwidth, typical frequency dependence of the main lobe direction is not obvious.

Table 2 Dimensions in millimetres of coax-to-SIW transition

d_s	1.52	l_{wg3}	1.73	y_c	3.63
l_{wg1}	5.71	w_{wg}	7.00		
l_{wg2}	3.34	x_c	0.44		

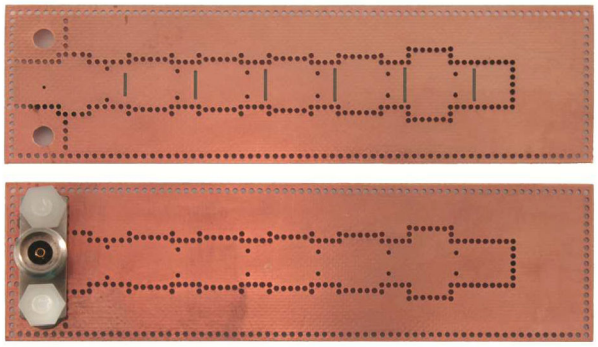

Fig. 9 *Fabricated prototype*

The antenna array is fed on the left side by a coaxial connector, representing a perpendicular coaxial-to-waveguide transition that is designed for the experimental verification. The details of this transition are shown in Fig. 8. We use a standard 2.92 mm connector (Pasternack PE44229) with a hermetic seal solder contact (PE1001-1). The position of the coaxial (x_c, y_c), the diameter of the coupling slot (d_s) and the waveguide discontinuity (l_{wg1}, l_{wg2}, l_{wg3}, w_{wg}) are the relevant parameters for minimising the input reflection coefficient of the antenna array. The coupling slot compensates for the inductance of the coaxial pin and the waveguide discontinuity operates as transmission line matching circuit. The resulting reflection coefficient of the antenna array at the coaxial input is presented in the next section. The geometry parameters of the transition are listed in Table 2.

3 Experimental results

For the prototype, the solid metal walls of the model were replaced by two opposite rows of metalised 0.60 mm via holes with a row-to-row distance of 5.58 mm (measured at row centre), exploiting an approach of [11]. The distance between consecutive vias was 0.86 mm. The fabricated prototype with an overall size of 20 mm × 73 mm is depicted in Fig. 9. Additional metalised via holes were deployed around the edge of the board. In this way, we eliminated the creation of half-mode SIWs around the board edge and ensured minimum parasitic radiation that could degrade the radiation pattern and increase SLLs. To ensure a good ground connection, the 2.92 mm connector with the solder contact was contacted to the bottom layer of the prototype by additionally using conductive epoxy resin. The centre pin was soldered to the top layer.

The measured reflection coefficient and gain in the perpendicular direction of the fabricated antenna array are depicted in Fig. 10. The bandwidth for −10 dB reflection was measured to be 150 MHz (24.12–24.27 GHz). The resonant frequency is slightly higher than the designed frequency of 24.125 GHz due to fabrication and material tolerances. The normalised radiation pattern (Fig. 11) was measured in both the *E*-plane and *H*-plane at the resonant frequency. The slightly increased SLL of −28 dB and the marginally wider main lobe of 30° for the 10 dB-beamwidth are in excellent agreement with the simulated values of −29.3 dB and 27°, respectively. The antenna array shows low cross-polarisation levels in both planes, which is characteristic for slot antenna arrays. The fabricated antenna array radiates in a perpendicular direction with a maximum gain of 11.6 dBi. The 0.8 dB difference with the simulated gain of 12.4 dBi is caused by slightly higher dielectric and metal losses of the used substrate. In addition, the measurement uncertainty of the gain measurement was ∼0.5 dB.

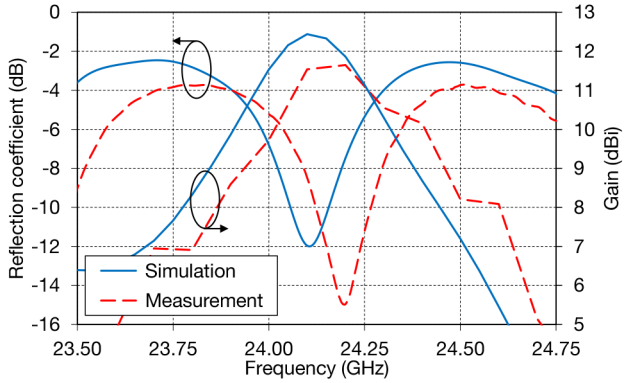

Fig. 10 *Reflection coefficient and gain in the perpendicular direction of the fabricated slot antenna array*

4 Conclusion

In this study, a novel basic antenna element for travelling wave SIW arrays has been proposed. The antenna element is based on a transverse slot, complemented by a pair of reflection-cancelling vias and a phase shifter. Compared to published travelling-wave transverse slot arrays [6, 8], the advantage of this different antenna element is in independent control the amplitude and phase of the radiated wave. To verify the performance of the proposed antenna element, we evaluated the concept for a six-element antenna array with −30 dB SLL, intended for a 24 GHz radar system. The fabricated prototype shows almost perfect agreement with the simulation results. Thanks to the possibility for phase adjusting of each antenna element, the presented design will be adopted in future work for shaped-beam patterns.

5 Acknowledgments

Research described in this paper was financed by the Czech Ministry of Education in the frame of the National Sustainability Program under grant LO1401. For research, the infrastructure of the SIX Center was used.

6 References

[1] Hosseininejad, S.E., Komjani, N.: 'Optimum design of traveling-wave SIW slot array antennas', *IEEE Trans. Antennas Propag.*, 2013, **61**, (4), pp. 1971–1975

[2] Zhao, C., Li, X., Sun, C., *et al.*: 'Design of a low-SLL SIW slot array antenna with a large declination in Ka-band', *IEEE Access*, 2019, **7**, pp. 120541–120547

[3] Zhang, L., Li, L., Yi, H.: 'Design of a traveling wave slot array on substrate integrated waveguide for 24 GHz traffic monitoring'. Proc. Cross Strait Quad-Regional Radio Science and Wireless Technology Conf., Xuzhou, China, 2018, pp. 1–3

[4] Qiu, L., Xiao, K., Chai, S.L., *et al.*: 'A double-layer shaped-beam traveling-wave slot array based on SIW', *IEEE Trans. Antennas Propag.*, 2016, **64**, (11), pp. 4639–4647

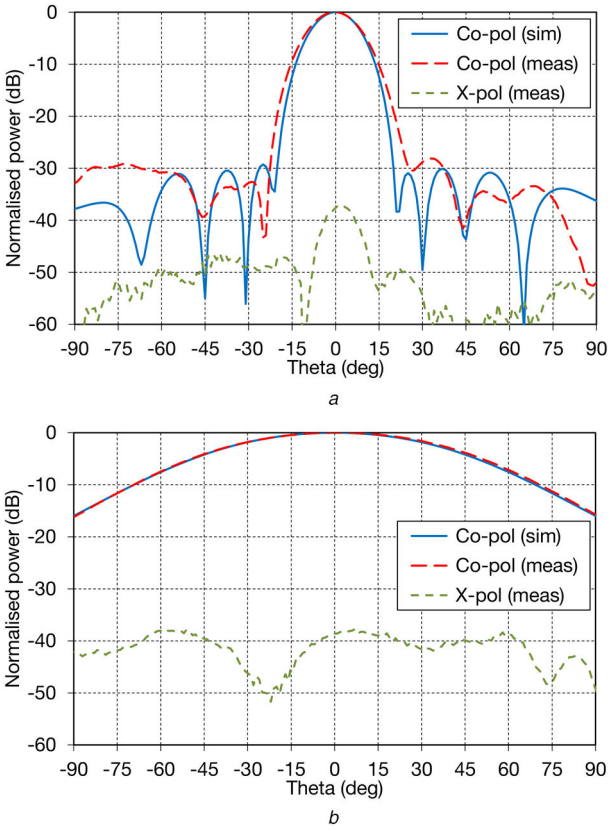

Fig. 11 *Radiation pattern of fabricated slot antenna array for co-polarisation (co-pol) and cross-polarisation (x-pol) at 24.2 GHz*
(a) *E*-plane, ***(b)*** *H*-plane

[5] Peters, F.D.L., Tatu, S.O., Denidni, T.A.: 'Design of traveling-wave equidistant slot antennas for millimeter-wave applications'. Proc. IEEE Int. Symp. on Antennas and Propagation, Spokane, WA, 2011, pp. 3037–3040

[6] Hirokawa, J., Kirita, M., Ando, M.: 'A linear array of transverse slots on a hollow waveguide with a layer of parasitic dipole-quartets for sidelobe suppression'. Proc. Asia-Pacific Microwave Conf., Bangkok, 2007, pp. 1–4

[7] Zhang, Q, Lu, Y.: 'A novel reflection-canceling design for substrate integrated waveguide based 45-degree linearly polarized slot antenna array'. Proc. IEEE Int. Symp. on Antennas and Propagation, San Diego, CA, USA, 2008, pp. 1–4

[8] Hirokawa, J., Yamazaki, C., Ando, M.: 'Postwall waveguide slot array with cosecant radiation pattern and null filling for base station antennas in local multidistributed systems', *Radio Sci.*, 2002, **37**, (2), pp. 1–7

[9] Elliott, R.: 'An improved design procedure for small arrays of shunt slots', *IEEE Trans. Antennas Propag.*, 1983, **31**, (1), pp. 48–53

[10] Vallecchi, A., Gentili, G.B.: 'Dual-polarized linear series-fed microstrip arrays with very low losses and cross polarization', *IEEE Antennas Wirel. Propag. Lett.*, 2004, **3**, pp. 123–126

[11] Yan, L., Hong, W., Wu, K., *et al.*: 'Investigations on the propagation characteristics of the substrate integrated waveguide based on the method of lines', *IEE Proc. Microw. Antennas Propag.*, 2005, **152**, (1), pp. 35–42